

Measurement of Branching Fractions of J/ψ and $\psi(3686)$ decays to Σ^+ and $\bar{\Sigma}^-$

M. Ablikim¹, M. N. Achasov^{10,b}, P. Adlarson⁶⁷, S. Ahmed¹⁵, M. Albrecht⁴, R. Aliberti²⁸, A. Amoroso^{66A,66C}, M. R. An³², Q. An^{63,49}, X. H. Bai⁵⁷, Y. Bai⁴⁸, O. Bakina²⁹, R. Baldini Ferroli^{23A}, I. Balossino^{24A}, Y. Ban^{38,h}, K. Begzsuren²⁶, N. Berger²⁸, M. Bertani^{23A}, D. Bettoni^{24A}, F. Bianchi^{66A,66C}, J. Bloms⁶⁰, A. Bortone^{66A,66C}, I. Boyko²⁹, R. A. Briere⁵, H. Cai⁶⁸, X. Cai^{1,49}, A. Calcaterra^{23A}, G. F. Cao^{1,54}, N. Cao^{1,54}, S. A. Cetin^{53A}, J. F. Chang^{1,49}, W. L. Chang^{1,54}, G. Chelkov^{29,a}, G. Chen¹, H. S. Chen^{1,54}, M. L. Chen^{1,49}, S. J. Chen³⁵, X. R. Chen²⁵, Y. B. Chen^{1,49}, Z. J. Chen^{20,i}, W. S. Cheng^{66C}, G. Cibinetto^{24A}, F. Cossio^{66C}, X. F. Cui³⁶, H. L. Dai^{1,49}, J. P. Dai^{42,e}, X. C. Dai^{1,54}, A. Dbeysi¹⁵, R. E. de Boer⁴, D. Dedovich²⁹, Z. Y. Deng¹, A. Denig²⁸, I. Denysenko²⁹, M. Destefanis^{66A,66C}, F. De Mori^{66A,66C}, Y. Ding³³, C. Dong³⁶, J. Dong^{1,49}, L. Y. Dong^{1,54}, M. Y. Dong^{1,49,54}, X. Dong⁶⁸, S. X. Du⁷¹, Y. L. Fan⁶⁸, J. Fang^{1,49}, S. S. Fang^{1,54}, Y. Fang¹, R. Farinelli^{24A}, L. Fava^{66B,66C}, F. Feldbauer⁴, G. Felici^{23A}, C. Q. Feng^{63,49}, J. H. Feng⁵⁰, M. Fritsch⁴, C. D. Fu¹, Y. Gao^{38,h}, Y. Gao^{63,49}, Y. Gao⁶⁴, I. Garzia^{24A,24B}, P. T. Ge⁶⁸, C. Geng⁵⁰, E. M. Gersabeck⁵⁸, A. Gilman⁶¹, K. Goetzen¹¹, L. Gong³³, W. X. Gong^{1,49}, W. Gradl²⁸, M. Greco^{66A,66C}, L. M. Gu³⁵, M. H. Gu^{1,49}, Y. T. Gu¹³, C. Y. Guan^{1,54}, A. Q. Guo²², L. B. Guo³⁴, R. P. Guo⁴⁰, Y. P. Guo^{9,f}, A. Guskov^{29,a}, T. T. Han⁴¹, W. Y. Han³², X. Q. Hao¹⁶, F. A. Harris⁵⁶, K. L. He^{1,54}, F. H. Heinsius⁴, C. H. Heinz²⁸, Y. K. Heng^{1,49,54}, C. Herold⁵¹, M. Himmelreich^{11,d}, T. Holtmann⁴, G. Y. Hou^{1,54}, Y. R. Hou⁵⁴, Z. L. Hou¹, H. M. Hu^{1,54}, J. F. Hu^{47,j}, T. Hu^{1,49,54}, Y. Hu¹, G. S. Huang^{63,49}, L. Q. Huang⁶⁴, X. T. Huang⁴¹, Y. P. Huang¹, Z. Huang^{38,h}, T. Hussain⁶⁵, N. Hüsken^{22,28}, W. Ikegami Andersson⁶⁷, W. Imoehl²², M. Irshad^{63,49}, S. Jaeger⁴, S. Janchiv²⁶, Q. Ji¹, Q. P. Ji¹⁶, X. B. Ji^{1,54}, X. L. Ji^{1,49}, Y. Y. Ji⁴¹, H. B. Jiang⁴¹, X. S. Jiang^{1,49,54}, J. B. Jiao⁴¹, Z. Jiao¹⁸, S. Jin³⁵, Y. Jin⁵⁷, M. Q. Jing^{1,54}, T. Johansson⁶⁷, N. Kalantar-Nayestanaki⁵⁵, X. S. Kang³³, R. Kappert⁵⁵, M. Kavatsyuk⁵⁵, B. C. Ke^{43,1}, I. K. Keshk⁴, A. Khoukaz⁶⁰, P. Kiese²⁸, R. Kiuchi¹, R. Kliemt¹¹, L. Koch³⁰, O. B. Kolcu^{53A}, B. Kopf⁴, M. Kuemmel⁴, M. Kuessner⁴, A. Kupsc⁶⁷, M. G. Kurth^{1,54}, W. Kühn³⁰, J. J. Lane⁵⁸, J. S. Lange³⁰, P. Larin¹⁵, A. Lavanina²¹, L. Lavezzi^{66A,66C}, Z. H. Lei^{63,49}, H. Leithoff²⁸, M. Lellmann²⁸, T. Lenz²⁸, C. Li³⁹, C. H. Li³², Cheng Li^{63,49}, D. M. Li⁷¹, F. Li^{1,49}, G. Li¹, H. Li^{63,49}, H. Li⁴³, H. B. Li^{1,54}, H. J. Li¹⁶, J. L. Li⁴¹, J. Q. Li⁴, J. S. Li⁵⁰, Ke Li¹, L. K. Li¹, Lei Li³, P. R. Li^{31,k,l}, S. Y. Li⁵², W. D. Li^{1,54}, W. G. Li¹, X. H. Li^{63,49}, X. L. Li⁴¹, Xiaoyu Li^{1,54}, Z. Y. Li⁵⁰, H. Liang^{1,54}, H. Liang²⁷, H. Liang^{63,49}, Y. F. Liang⁴⁵, Y. T. Liang²⁵, G. R. Liao¹², L. Z. Liao^{1,54}, J. Libby²¹, A. Limphirat⁵¹, C. X. Lin⁵⁰, T. Lin¹, B. J. Liu¹, C. X. Liu¹, D. Liu^{15,63}, F. H. Liu⁴⁴, Fang Liu¹, Feng Liu⁶, H. B. Liu¹³, H. M. Liu^{1,54}, Huanhuan Liu¹, Huihui Liu¹⁷, J. B. Liu^{63,49}, J. L. Liu⁶⁴, J. Y. Liu^{1,54}, K. Liu¹, K. Y. Liu³³, L. Liu^{63,49}, M. H. Liu^{9,f}, P. L. Liu¹, Q. Liu⁶⁸, Q. Liu⁵⁴, S. B. Liu^{63,49}, Shuai Liu⁴⁶, T. Liu^{9,f}, T. Liu^{1,54}, W. M. Liu^{63,49}, X. Liu^{31,k,l}, Y. Liu^{31,k,l}, Y. B. Liu³⁶, Z. A. Liu^{1,49,54}, Z. Q. Liu⁴¹, X. C. Lou^{1,49,54}, F. X. Lu⁵⁰, H. J. Lu¹⁸, J. D. Lu^{1,54}, J. G. Lu^{1,49}, X. L. Lu¹, Y. Lu¹, Y. P. Lu^{1,49}, C. L. Luo³⁴, M. X. Luo⁷⁰, P. W. Luo⁵⁰, T. Luo^{9,f}, X. L. Luo^{1,49}, X. R. Lyu⁵⁴, F. C. Ma³³, H. L. Ma¹, L. L. Ma⁴¹,

M. M. Ma^{1,54}, Q. M. Ma¹, R. Q. Ma^{1,54}, R. T. Ma⁵⁴, X. X. Ma^{1,54}, X. Y. Ma^{1,49}, Y. Ma^{38,h},
 F. E. Maas¹⁵, M. Maggiora^{66A,66C}, S. Maldaner⁴, S. Malde⁶¹, Q. A. Malik⁶⁵, A. Mangoni^{23B},
 Y. J. Mao^{38,h}, Z. P. Mao¹, S. Marcello^{66A,66C}, Z. X. Meng⁵⁷, J. G. Messchendorp⁵⁵,
 G. Mezzadri^{24A}, T. J. Min³⁵, R. E. Mitchell²², X. H. Mo^{1,49,54}, N. Yu. Muchnoi^{10,b},
 H. Muramatsu⁵⁹, S. Nakhoul^{11,d}, Y. Nefedov²⁹, F. Nerling^{11,d}, I. B. Nikolaev^{10,b}, Z. Ning^{1,49},
 S. Nisar^{8,g}, S. L. Olsen⁵⁴, Q. Ouyang^{1,49,54}, S. Pacetti^{23B,23C}, X. Pan^{9,f}, Y. Pan⁵⁸,
 A. Pathak¹, A. Pathak²⁷, P. Patteri^{23A}, M. Pelizaeus⁴, H. P. Peng^{63,49}, K. Peters^{11,d},
 J. Pettersson⁶⁷, J. L. Ping³⁴, R. G. Ping^{1,54}, S. Pogodin²⁹, R. Poling⁵⁹, V. Prasad^{63,49},
 H. Qi^{63,49}, H. R. Qi⁵², K. H. Qi²⁵, M. Qi³⁵, T. Y. Qi^{9,f}, S. Qian^{1,49}, W. B. Qian⁵⁴, Z. Qian⁵⁰,
 C. F. Qiao⁵⁴, L. Q. Qin¹², X. P. Qin^{9,f}, X. S. Qin⁴¹, Z. H. Qin^{1,49}, J. F. Qiu¹, S. Q. Qu³⁶,
 K. H. Rashid⁶⁵, K. Ravindran²¹, C. F. Redmer²⁸, A. Rivetti^{66C}, V. Rodin⁵⁵, M. Rolo^{66C},
 G. Rong^{1,54}, Ch. Rosner¹⁵, M. Rump⁶⁰, H. S. Sang⁶³, A. Sarantsev^{29,c}, Y. Schelhaas²⁸,
 C. Schnier⁴, K. Schoenning⁶⁷, M. Scodreggio^{24A,24B}, D. C. Shan⁴⁶, W. Shan¹⁹,
 X. Y. Shan^{63,49}, J. F. Shangquan⁴⁶, M. Shao^{63,49}, C. P. Shen^{9,f}, H. F. Shen^{1,54}, P. X. Shen³⁶,
 X. Y. Shen^{1,54}, H. C. Shi^{63,49}, R. S. Shi^{1,54}, X. Shi^{1,49}, X. D Shi^{63,49}, W. M. Song^{27,1},
 Y. X. Song^{38,h}, S. Sosio^{66A,66C}, S. Spataro^{66A,66C}, K. X. Su⁶⁸, P. P. Su⁴⁶, G. X. Sun¹,
 H. K. Sun¹, J. F. Sun¹⁶, L. Sun⁶⁸, S. S. Sun^{1,54}, T. Sun^{1,54}, W. Y. Sun³⁴, W. Y. Sun²⁷,
 X Sun^{20,i}, Y. J. Sun^{63,49}, Y. Z. Sun¹, Z. T. Sun¹, Y. H. Tan⁶⁸, Y. X. Tan^{63,49}, C. J. Tang⁴⁵,
 G. Y. Tang¹, J. Tang⁵⁰, J. X. Teng^{63,49}, V. Thoren⁶⁷, W. H. Tian⁴³, Y. T. Tian²⁵,
 I. Uman^{53B}, B. Wang¹, C. W. Wang³⁵, D. Y. Wang^{38,h}, H. J. Wang^{31,k,l}, H. P. Wang^{1,54},
 K. Wang^{1,49}, L. L. Wang¹, M. Wang⁴¹, M. Z. Wang^{38,h}, Meng Wang^{1,54}, S. Wang^{9,f},
 W. Wang⁵⁰, W. H. Wang⁶⁸, W. P. Wang^{63,49}, X. Wang^{38,h}, X. F. Wang^{31,k,l}, X. L. Wang^{9,f},
 Y. Wang^{63,49}, Y. Wang⁵⁰, Y. D. Wang³⁷, Y. F. Wang^{1,49,54}, Y. Q. Wang¹, Y. Y. Wang^{31,k,l},
 Z. Wang^{1,49}, Z. Y. Wang¹, Ziyi Wang⁵⁴, Zongyuan Wang^{1,54}, D. H. Wei¹², F. Weidner⁶⁰,
 S. P. Wen¹, D. J. White⁵⁸, U. Wiedner⁴, G. Wilkinson⁶¹, M. Wolke⁶⁷, L. Wollenberg⁴,
 J. F. Wu^{1,54}, L. H. Wu¹, L. J. Wu^{1,54}, X. Wu^{9,f}, Z. Wu^{1,49}, L. Xia^{63,49}, T. Xiang^{38,h},
 H. Xiao^{9,f}, S. Y. Xiao¹, Z. J. Xiao³⁴, X. H. Xie^{38,h}, Y. G. Xie^{1,49}, Y. H. Xie⁶, T. Y. Xing^{1,54},
 C. J. Xu⁵⁰, G. F. Xu¹, Q. J. Xu¹⁴, W. Xu^{1,54}, X. P. Xu⁴⁶, Y. C. Xu⁵⁴, F. Yan^{9,f}, L. Yan^{9,f},
 W. B. Yan^{63,49}, W. C. Yan⁷¹, Xu Yan⁴⁶, H. J. Yang^{42,e}, H. X. Yang¹, L. Yang⁴³, S. L. Yang⁵⁴,
 Y. X. Yang¹², Yifan Yang^{1,54}, Zhi Yang²⁵, M. Ye^{1,49}, M. H. Ye⁷, J. H. Yin¹, Z. Y. You⁵⁰,
 B. X. Yu^{1,49,54}, C. X. Yu³⁶, G. Yu^{1,54}, J. S. Yu^{20,i}, T. Yu⁶⁴, C. Z. Yuan^{1,54}, L. Yuan²,
 X. Q. Yuan^{38,h}, Y. Yuan¹, Z. Y. Yuan⁵⁰, C. X. Yue³², A. A. Zafar⁶⁵, X. Zeng Zeng⁶,
 Y. Zeng^{20,i}, A. Q. Zhang¹, B. X. Zhang¹, G. Y. Zhang¹⁶, H. Zhang⁶³, H. H. Zhang⁵⁰,
 H. H. Zhang²⁷, H. Y. Zhang^{1,49}, J. L. Zhang⁶⁹, J. Q. Zhang³⁴, J. W. Zhang^{1,49,54},
 J. Y. Zhang¹, J. Z. Zhang^{1,54}, Jianyu Zhang^{1,54}, Jiawei Zhang^{1,54}, L. M. Zhang⁵²,
 L. Q. Zhang⁵⁰, Lei Zhang³⁵, S. Zhang⁵⁰, S. F. Zhang³⁵, Shulei Zhang^{20,i}, X. D. Zhang³⁷,
 X. Y. Zhang⁴¹, Y. Zhang⁶¹, Y. T. Zhang⁷¹, Y. H. Zhang^{1,49}, Yan Zhang^{63,49}, Yao Zhang¹,
 Z. Y. Zhang⁶⁸, G. Zhao¹, J. Zhao³², J. Y. Zhao^{1,54}, J. Z. Zhao^{1,49}, Lei Zhao^{63,49}, Ling Zhao¹,
 M. G. Zhao³⁶, Q. Zhao¹, S. J. Zhao⁷¹, Y. B. Zhao^{1,49}, Y. X. Zhao²⁵, Z. G. Zhao^{63,49},
 A. Zhemchugov^{29,a}, B. Zheng⁶⁴, J. P. Zheng^{1,49}, Y. H. Zheng⁵⁴, B. Zhong³⁴, C. Zhong⁶⁴,
 L. P. Zhou^{1,54}, Q. Zhou^{1,54}, X. Zhou⁶⁸, X. K. Zhou⁵⁴, X. R. Zhou^{63,49}, X. Y. Zhou³²,
 A. N. Zhu^{1,54}, J. Zhu³⁶, K. Zhu¹, K. J. Zhu^{1,49,54}, S. H. Zhu⁶², T. J. Zhu⁶⁹, W. J. Zhu³⁶,
 W. J. Zhu^{9,f}, Y. C. Zhu^{63,49}, Z. A. Zhu^{1,54}, B. S. Zou¹, J. H. Zou¹

(BESIII Collaboration)

¹ Institute of High Energy Physics, Beijing 100049, People's Republic of China

² Beihang University, Beijing 100191, People's Republic of China

- ³ *Beijing Institute of Petrochemical Technology, Beijing 102617, People's Republic of China*
- ⁴ *Bochum Ruhr-University, D-44780 Bochum, Germany*
- ⁵ *Carnegie Mellon University, Pittsburgh, Pennsylvania 15213, USA*
- ⁶ *Central China Normal University, Wuhan 430079, People's Republic of China*
- ⁷ *China Center of Advanced Science and Technology, Beijing 100190, People's Republic of China*
- ⁸ *COMSATS University Islamabad, Lahore Campus, Defence Road, Off Raiwind Road, 54000 Lahore, Pakistan*
- ⁹ *Fudan University, Shanghai 200443, People's Republic of China*
- ¹⁰ *G.I. Budker Institute of Nuclear Physics SB RAS (BINP), Novosibirsk 630090, Russia*
- ¹¹ *GSI Helmholtzcentre for Heavy Ion Research GmbH, D-64291 Darmstadt, Germany*
- ¹² *Guangxi Normal University, Guilin 541004, People's Republic of China*
- ¹³ *Guangxi University, Nanning 530004, People's Republic of China*
- ¹⁴ *Hangzhou Normal University, Hangzhou 310036, People's Republic of China*
- ¹⁵ *Helmholtz Institute Mainz, Staudinger Weg 18, D-55099 Mainz, Germany*
- ¹⁶ *Henan Normal University, Xinxiang 453007, People's Republic of China*
- ¹⁷ *Henan University of Science and Technology, Luoyang 471003, People's Republic of China*
- ¹⁸ *Huangshan College, Huangshan 245000, People's Republic of China*
- ¹⁹ *Hunan Normal University, Changsha 410081, People's Republic of China*
- ²⁰ *Hunan University, Changsha 410082, People's Republic of China*
- ²¹ *Indian Institute of Technology Madras, Chennai 600036, India*
- ²² *Indiana University, Bloomington, Indiana 47405, USA*
- ²³ *INFN Laboratori Nazionali di Frascati , (A)INFN Laboratori Nazionali di Frascati, I-00044, Frascati, Italy; (B)INFN Sezione di Perugia, I-06100, Perugia, Italy; (C)University of Perugia, I-06100, Perugia, Italy*
- ²⁴ *INFN Sezione di Ferrara, (A)INFN Sezione di Ferrara, I-44122, Ferrara, Italy; (B)University of Ferrara, I-44122, Ferrara, Italy*
- ²⁵ *Institute of Modern Physics, Lanzhou 730000, People's Republic of China*
- ²⁶ *Institute of Physics and Technology, Peace Ave. 54B, Ulaanbaatar 13330, Mongolia*
- ²⁷ *Jilin University, Changchun 130012, People's Republic of China*
- ²⁸ *Johannes Gutenberg University of Mainz, Johann-Joachim-Becher-Weg 45, D-55099 Mainz, Germany*
- ²⁹ *Joint Institute for Nuclear Research, 141980 Dubna, Moscow region, Russia*
- ³⁰ *Justus-Liebig-Universitaet Giessen, II. Physikalisches Institut, Heinrich-Buff-Ring 16, D-35392 Giessen, Germany*
- ³¹ *Lanzhou University, Lanzhou 730000, People's Republic of China*
- ³² *Liaoning Normal University, Dalian 116029, People's Republic of China*
- ³³ *Liaoning University, Shenyang 110036, People's Republic of China*
- ³⁴ *Nanjing Normal University, Nanjing 210023, People's Republic of China*
- ³⁵ *Nanjing University, Nanjing 210093, People's Republic of China*
- ³⁶ *Nankai University, Tianjin 300071, People's Republic of China*
- ³⁷ *North China Electric Power University, Beijing 102206, People's Republic of China*
- ³⁸ *Peking University, Beijing 100871, People's Republic of China*
- ³⁹ *Qufu Normal University, Qufu 273165, People's Republic of China*
- ⁴⁰ *Shandong Normal University, Jinan 250014, People's Republic of China*
- ⁴¹ *Shandong University, Jinan 250100, People's Republic of China*
- ⁴² *Shanghai Jiao Tong University, Shanghai 200240, People's Republic of China*
- ⁴³ *Shanxi Normal University, Linfen 041004, People's Republic of China*
- ⁴⁴ *Shanxi University, Taiyuan 030006, People's Republic of China*

- ⁴⁵ *Sichuan University, Chengdu 610064, People's Republic of China*
- ⁴⁶ *Soochow University, Suzhou 215006, People's Republic of China*
- ⁴⁷ *South China Normal University, Guangzhou 510006, People's Republic of China*
- ⁴⁸ *Southeast University, Nanjing 211100, People's Republic of China*
- ⁴⁹ *State Key Laboratory of Particle Detection and Electronics, Beijing 100049, Hefei 230026, People's Republic of China*
- ⁵⁰ *Sun Yat-Sen University, Guangzhou 510275, People's Republic of China*
- ⁵¹ *Suranaree University of Technology, University Avenue 111, Nakhon Ratchasima 30000, Thailand*
- ⁵² *Tsinghua University, Beijing 100084, People's Republic of China*
- ⁵³ *Turkish Accelerator Center Particle Factory Group, (A)Istinye University, 34010, Istanbul, Turkey; (B)Near East University, Nicosia, North Cyprus, Mersin 10, Turkey*
- ⁵⁴ *University of Chinese Academy of Sciences, Beijing 100049, People's Republic of China*
- ⁵⁵ *University of Groningen, NL-9747 AA Groningen, The Netherlands*
- ⁵⁶ *University of Hawaii, Honolulu, Hawaii 96822, USA*
- ⁵⁷ *University of Jinan, Jinan 250022, People's Republic of China*
- ⁵⁸ *University of Manchester, Oxford Road, Manchester, M13 9PL, United Kingdom*
- ⁵⁹ *University of Minnesota, Minneapolis, Minnesota 55455, USA*
- ⁶⁰ *University of Muenster, Wilhelm-Klemm-Str. 9, 48149 Muenster, Germany*
- ⁶¹ *University of Oxford, Keble Rd, Oxford, UK OX13RH*
- ⁶² *University of Science and Technology Liaoning, Anshan 114051, People's Republic of China*
- ⁶³ *University of Science and Technology of China, Hefei 230026, People's Republic of China*
- ⁶⁴ *University of South China, Hengyang 421001, People's Republic of China*
- ⁶⁵ *University of the Punjab, Lahore-54590, Pakistan*
- ⁶⁶ *University of Turin and INFN, (A)University of Turin, I-10125, Turin, Italy; (B)University of Eastern Piedmont, I-15121, Alessandria, Italy; (C)INFN, I-10125, Turin, Italy*
- ⁶⁷ *Uppsala University, Box 516, SE-75120 Uppsala, Sweden*
- ⁶⁸ *Wuhan University, Wuhan 430072, People's Republic of China*
- ⁶⁹ *Xinyang Normal University, Xinyang 464000, People's Republic of China*
- ⁷⁰ *Zhejiang University, Hangzhou 310027, People's Republic of China*
- ⁷¹ *Zhengzhou University, Zhengzhou 450001, People's Republic of China*
- ^a *Also at the Moscow Institute of Physics and Technology, Moscow 141700, Russia*
- ^b *Also at the Novosibirsk State University, Novosibirsk, 630090, Russia*
- ^c *Also at the NRC "Kurchatov Institute", PNPI, 188300, Gatchina, Russia*
- ^d *Also at Goethe University Frankfurt, 60323 Frankfurt am Main, Germany*
- ^e *Also at Key Laboratory for Particle Physics, Astrophysics and Cosmology, Ministry of Education; Shanghai Key Laboratory for Particle Physics and Cosmology; Institute of Nuclear and Particle Physics, Shanghai 200240, People's Republic of China*
- ^f *Also at Key Laboratory of Nuclear Physics and Ion-beam Application (MOE) and Institute of Modern Physics, Fudan University, Shanghai 200443, People's Republic of China*
- ^g *Also at Harvard University, Department of Physics, Cambridge, MA, 02138, USA*
- ^h *Also at State Key Laboratory of Nuclear Physics and Technology, Peking University, Beijing 100871, People's Republic of China*
- ⁱ *Also at School of Physics and Electronics, Hunan University, Changsha 410082, China*
- ^j *Also at Guangdong Provincial Key Laboratory of Nuclear Science, Institute of Quantum Matter, South China Normal University, Guangzhou 510006, China*
- ^k *Also at Frontiers Science Center for Rare Isotopes, Lanzhou University, Lanzhou 730000, People's Republic of China*

^l Also at Lanzhou Center for Theoretical Physics, Lanzhou University, Lanzhou 730000, People's Republic of China

ABSTRACT: Using 1310.6×10^6 J/ψ and 448.1×10^6 $\psi(3686)$ events collected with the BESIII detector, the branching fractions of J/ψ decays to $\Sigma^+\bar{\Sigma}^-$ is measured to be $(10.61 \pm 0.04 \pm 0.36) \times 10^{-4}$, which is significantly more precise than the current world average. The branching fractions of $\psi(3686)$ decays to $\Sigma^+\bar{\Sigma}^-$ is measured to be $(2.52 \pm 0.04 \pm 0.09) \times 10^{-4}$, which is consistent with the previous measurements. In addition, the ratio of $\mathcal{B}(\psi(3686) \rightarrow \Sigma^+\bar{\Sigma}^-)/\mathcal{B}(J/\psi \rightarrow \Sigma^+\bar{\Sigma}^-)$ is determined to be $(23.8 \pm 1.1)\%$ which violates the “12% rule”.

Contents

1	Introduction	1
2	BESIII Detector and Monte Carlo Simulation	2
3	Selection criteria	3
4	Branching fraction measurements	5
5	Systematic Uncertainties	7
5.1	MC efficiency correction for charged tracks	8
5.2	π^0 efficiency correction	8
5.3	Decay parameters	8
5.4	Fitting function	8
5.5	Background estimation	9
5.6	$M(\bar{p}\pi^0)$ mass window selection	9
5.7	Kinematic fitting	9
5.8	Branching fractions and numbers of J/ψ and $\psi(3686)$	9
6	Summary	9

1 Introduction

Measurements on the decays of J/ψ and $\psi(3686)$ (denoted here collectively as Ψ) can be used to study flavor-SU(3) symmetry breaking and test quantum chromodynamics (QCD) in the perturbative energy regime [1]. If we consider J/ψ decays into $B_8\bar{B}_8$ and $B_{10}\bar{B}_{10}$ final states, where B_8 and B_{10} represent the baryon octet and decuplet states, respectively, and if the electromagnetic contributions are neglected, flavor-SU(3) symmetry gives the same decay amplitudes for all J/ψ decays to baryon anti-baryon pairs. However, broken flavor-SU(3) symmetry can contribute to the differences in branching fractions of different baryonic pairs. Furthermore, the branching fractions are determined not only by strong interaction amplitudes, but also by electromagnetic interactions and interferences between them [2], although these are much smaller than the expected flavor-SU(3) breaking effects. As shown in Table 1, a phenomenologically plausible model [3, 4] can be made to fit the pattern of branching fractions of J/ψ decays to baryon octet final states well [5]. However the precision on the branching fraction of $J/\psi \rightarrow \Sigma^+\bar{\Sigma}^-$ is still relatively poor [6]. The 1310.6×10^6 J/ψ event sample collected by the BESIII experiment in 2009 and 2012 allows a much more precise measurement of the branching fraction of $J/\psi \rightarrow \Sigma^+\bar{\Sigma}^-$.

According to pQCD, the ratio of Γ_h to Γ_l , where Γ_h is the partial width of J/ψ ($\psi(3686)$) decay to light hadrons and Γ_l is the partial width to leptons, does not depend on the particle

Table 1. Comparison of the experimental measurements (\mathcal{B}_{pdg}) [5] and phenomenological calculations (\mathcal{B}_{cal}) [3, 4] for the branching fractions of J/ψ decays to baryon octet final states, where $\Delta(\sigma)$ is the difference in terms of the total uncertainty. Dash (–) represents no experimental measurement.

$B\bar{B}$	$\mathcal{B}_{\text{pdg}}(10^{-3})$	$\mathcal{B}_{\text{cal}}(10^{-3})$	$\Delta(\sigma)$
$\Sigma^0\bar{\Sigma}^0$	1.164 ± 0.004	1.160 ± 0.041	~ 0.09
$\Lambda\bar{\Lambda}$	1.943 ± 0.003	1.940 ± 0.055	~ 0.05
$\Lambda\bar{\Sigma}^0 + \text{c.c.}$	0.0283 ± 0.0023	0.0280 ± 0.0024	~ 0.06
$p\bar{p}$	2.121 ± 0.029	2.10 ± 0.16	~ 0.1
$n\bar{n}$	2.09 ± 0.16	2.10 ± 0.12	~ 0.04
$\Sigma^+\bar{\Sigma}^-$	1.50 ± 0.24	1.110 ± 0.086	~ 1
$\Sigma^-\bar{\Sigma}^+$	–	0.857 ± 0.051	–
$\Xi^0\bar{\Xi}^0$	1.17 ± 0.04	1.180 ± 0.072	~ 0.09
$\Xi^-\bar{\Xi}^+$	0.97 ± 0.08	0.979 ± 0.065	~ 0.06

wave function [7]. The ratio between the branching fractions of J/ψ and $\psi(3686)$ decays to the same final states obeys the so-called “12% rule”,

$$\frac{\mathcal{B}_{\psi(3686) \rightarrow h}}{\mathcal{B}_{J/\psi \rightarrow h}} \approx \frac{\mathcal{B}_{\psi(3686) \rightarrow l^+l^-}}{\mathcal{B}_{J/\psi \rightarrow l^+l^-}} = (13.3 \pm 0.3)\%.$$

Although a large fraction of exclusive decay channels follow the rule approximately, significant violation was first observed in the $\rho\pi$ channel [8]. The ratio of $\mathcal{B}(\psi(3686) \rightarrow \rho\pi)$ to $\mathcal{B}(J/\psi \rightarrow \rho\pi)$ is much smaller than the pQCD prediction, and this is called the “ $\rho\pi$ ” puzzle. To understand the “ $\rho\pi$ ” puzzle, the theoretical and experimental efforts have been made: amongst the suggested solutions are J/ψ -glueball admixture scheme, Intrinsic-charm-component scheme, Sequential-fragmentation model, Exponential-form-factor model, S-D wave mixing scheme, Final state interaction scheme and so on [9]. But there are no satisfactory explanations for all existing experimental results. Tests of the 12% rule using the baryonic decay modes may be helpful in understanding the $\rho\pi$ puzzle. With CLEO data [10, 11], the branching fraction of $\psi(3686) \rightarrow \Sigma^+\bar{\Sigma}^-$ was determined to be $(2.32 \pm 0.12) \times 10^{-4}$. The BESIII experiment, having collected the largest sample of $\psi(3686)$ events, gives the opportunity to improve the precision of this branching fraction and test the 12% rule.

In this paper we report, with improved precision, the branching fraction measurements of $J/\psi \rightarrow \Sigma^+\bar{\Sigma}^-$ and $\psi(3686) \rightarrow \Sigma^+\bar{\Sigma}^-$ based on 1310.6×10^6 J/ψ and 448.1×10^6 $\psi(3686)$ events collected with the BESIII detector at the BEPCII collider during 2009 and 2012.

2 BESIII Detector and Monte Carlo Simulation

The BESIII detector [12] records symmetric e^+e^- collisions provided by the BEPCII storage ring [13], which operates with a peak luminosity of $1 \times 10^{33} \text{ cm}^{-2}\text{s}^{-1}$ in the center-of-mass energy range from 2.0 to 4.9 GeV. BESIII has collected large data samples in this energy region [14]. The cylindrical core of the BESIII detector covers 93% of the full solid

angle and consists of a helium-based multilayer drift chamber (MDC), a plastic scintillator time-of-flight system (TOF), and a CsI(Tl) electromagnetic calorimeter (EMC), which are all enclosed in a superconducting solenoidal magnet providing a 1.0 T (0.9 T in 2012) magnetic field. The solenoid is supported by an octagonal flux-return yoke with resistive plate counter muon identification modules interleaved with steel. The charged-particle momentum resolution at 1 GeV/ c is 0.5%, and the dE/dx resolution is 6% for electrons from Bhabha scattering. The EMC measures photon energies with a resolution of 2.5% (5%) at 1 GeV in the barrel (end cap) region. The time resolution in the TOF barrel region is 68 ps, while that in the end cap region is 110 ps.

Monte Carlo (MC) simulated events are used to determine the detection efficiency, optimize selection criteria, and study possible backgrounds. GEANT4-based [15] MC simulation software, which includes the geometric and material descriptions of the BESIII detector, the detector response, and digitization models as well as the detector running conditions and performance, is used to generate MC samples. The simulation models the beam energy spread and initial state radiation (ISR) in the e^+e^- annihilations with the generator KKMC [16]. The inclusive MC samples of J/ψ and $\psi(3686)$ includes the production of the J/ψ and $\psi(3686)$ resonances, the ISR production of the J/ψ , and the continuum processes incorporated in KKMC. The known decay modes are modelled with EVTGEN [17] using branching fractions taken from the Particle Data Group [18], and the remaining unknown charmonium decays are modelled with LUNDCHARM [19]. Final state radiation (FSR) from charged final state particles is incorporated using the PHOTOS package [20]. To describe the MC simulation of the signal process, the differential cross section is expressed with respect to five observables $\xi = (\theta_{\Sigma^+}, \theta_p, \phi_p, \theta_{\bar{p}}, \phi_{\bar{p}})$ [21]. Here θ_{Σ^+} is the angle between the Σ^+ and electron (e^-) beam in the interaction center-of-mass frame (CM), θ_p, ϕ_p and $\theta_{\bar{p}}, \phi_{\bar{p}}$ are the polar and azimuthal angles of the proton and anti-proton measured in the rest frames of their corresponding mother particles. The parameters in the differential cross sections have been determined in Ref. [22].

3 Selection criteria

Candidates of $\Psi \rightarrow \Sigma^+\bar{\Sigma}^-$, where $\Sigma^+(\bar{\Sigma}^-) \rightarrow p\pi^0(\bar{p}\pi^0)$ and $\pi^0 \rightarrow \gamma\gamma$ are required to have two charged tracks with opposite charges and at least four photons. Charged tracks are required to be within the acceptance of the MDC. For each track, the point of closest approach to the interaction point must be within 2 cm in the plane perpendicular to the z axis and within ± 10 cm along z , where z is along the symmetry axis of the MDC. A particle identification algorithm (PID) combines measurements of the energy deposited in the MDC (dE/dx) and the flight time to the TOF to form likelihoods $\mathcal{L}(h)$ ($h = p, K, \pi$) for each hadron hypothesis. The two good charged tracks are identified as proton and anti-proton by requiring $\mathcal{L}(p) > \mathcal{L}(\pi)$ and $\mathcal{L}(p) > \mathcal{L}(K)$.

Photon candidates are reconstructed from isolated showers in the EMC. Each photon candidate is required to have a minimum energy of 25 MeV in the EMC barrel region or 50 MeV in the end cap region. To improve the reconstruction efficiency and the energy resolution, the energy deposited in the nearby TOF counters is included in the photon re-

construction. To suppress electronic noise and showers unrelated to the event, the difference between the EMC time and the event start time is required to be within $[0, 700]$ ns. The π^0 candidates are reconstructed by requiring the invariant mass of photon pairs to satisfy $(M_{\pi^0} - 60) < M_{\gamma\gamma} < (M_{\pi^0} + 40)$ MeV/ c^2 , where M_{π^0} is the nominal mass of π^0 [18]. The asymmetrical mass window is used because the photon energy deposited in the EMC has a tail on the low energy side. A one-constraint (1C) kinematic fit is performed on the photon pairs by constraining their invariant masses to the nominal π^0 mass, and the χ_{1C}^2 is required to be less than 25 to remove fake candidates. Further there must be at least two reconstructed π^0 candidates.

To further remove potential background events and improve the mass resolution, a four-constraint (4C) kinematic fit is performed, constraining the total reconstructed four momentum to that of the initial e^+e^- state. A requirement on the quality of the 4C kinematic fit of $\chi_{4C}^2 < 100$ is imposed, which is chosen by optimizing the figure-of-merit, defined as $\frac{S}{\sqrt{S+B}}$, where S is the number of signal events and B is the number of background events, which are estimated based on MC simulations. If the number of π^0 candidates in an event is greater than two, the $p\bar{p}\pi^0\pi^0$ combination with the lowest χ_{4C}^2 is selected. After kinematic fitting, the Σ^+ and $\bar{\Sigma}^-$ candidates are constructed from the proton, anti-proton and neutral-pion candidates, and the combination that minimizes $\sqrt{(M_{p\pi^0} - m_{\Sigma^+})^2 + (M_{\bar{p}\pi^0} - m_{\bar{\Sigma}^-})^2}$ is chosen in order to match the neutral pions to the corresponding baryons. For the $\psi(3686) \rightarrow \Sigma^+\bar{\Sigma}^-$ decay, an additional invariant mass requirement is imposed on the proton-antiproton pair, $|M_{p\bar{p}} - 3.1| > 0.05$ GeV/ c^2 , to remove the background of $\psi(3686) \rightarrow \pi^0\pi^0 J/\psi$ with $J/\psi \rightarrow p\bar{p}$.

To investigate other possible background processes, inclusive MC samples of 1.2×10^9 J/ψ and 5.06×10^8 $\psi(3686)$ decays are used and examined TopoAna, a software tool to categorise backgrounds and identify the physics processes of interests from the inclusive MC samples [23]. For $J/\psi \rightarrow \Sigma^+\bar{\Sigma}^-$, the dominant background contributions are found to be $J/\psi \rightarrow \Delta^+\bar{\Delta}^-$, $J/\psi \rightarrow p\bar{p}\pi^0\pi^0$, $J/\psi \rightarrow \gamma\Sigma^+\bar{\Sigma}^-$ and $J/\psi \rightarrow \gamma\eta_c$ with subsequent decay $\eta_c \rightarrow \Sigma^+\bar{\Sigma}^-$. For the $\psi(3686) \rightarrow \Sigma^+\bar{\Sigma}^-$, the main background contributions are from $\psi(3686) \rightarrow \Delta^+\bar{\Delta}^-$, $\psi(3686) \rightarrow p\bar{p}\pi^0\pi^0$, $\psi(3686) \rightarrow \gamma\chi_{c2}$ with $\chi_{c2} \rightarrow p\bar{p}\pi^0$ and $\psi(3686) \rightarrow \gamma\eta_c$ with $\eta_c \rightarrow \Sigma^+\bar{\Sigma}^-$. All the above backgrounds can be classified as peaking backgrounds or non-peaking backgrounds depending on whether there is $\Sigma^+\bar{\Sigma}^-$ in the final states. The peaking background contributions are estimated to be less than 0.1% of the signal and can thus be neglected. For non-peaking backgrounds, we treat them as a smooth distribution in the invariant mass spectrum. The sideband method is used to further check the background distributions. The signal region is defined as $1.17 < M_{p\pi^0/\bar{p}\pi^0} < 1.2$ GeV/ c^2 , and the lower and upper sideband regions are defined as $1.14 < M_{p\pi^0/\bar{p}\pi^0} < 1.155$ GeV/ c^2 and $1.225 < M_{p\pi^0/\bar{p}\pi^0} < 1.24$ GeV/ c^2 , respectively. The $M_{p\pi^0}$ distributions, shown in Fig 1(a)(b), are plotted by requiring $M_{\bar{p}\pi^0}$ to be within the signal or sideband region. Similarly, in Fig 1(c)(d), the $M_{\bar{p}\pi^0}$ distributions are plotted by requiring $M_{p\pi^0}$ to be within the signal or sideband region. There are no obvious peaking background contributions in the sideband region.

To investigate the contributions from the quantum electrodynamics (QED) process

of $e^+e^- \rightarrow \Sigma^+\bar{\Sigma}^-$, two continuum datasets collected at center-of-mass energies of 3.08 GeV and 3.65 GeV, with luminosities of 30 pb^{-1} and 44 pb^{-1} , are used. The absolute magnitude is determined according to the formula $N = N_{\text{continuum}}^{\text{survived}} \cdot \frac{\mathcal{L}_{\psi(3686)}}{\mathcal{L}_{\text{continuum}}} \cdot \frac{3.65^2}{3.686^2}$, where $N_{\text{continuum}}^{\text{survived}} = 2$ is the number of events which remained in the off-resonance sample after applying the same selection criteria, $\mathcal{L}_{\psi(3686)} = 668.55 \text{ pb}^{-1}$ and $\mathcal{L}_{\text{continuum}} = 44 \text{ pb}^{-1}$. The contribution of QED process is negligible for our measurement.

4 Branching fraction measurements

With the above selection criteria, there are significant enhancements close to the Σ^+ and $\bar{\Sigma}^-$ nominal masses in the two dimensional distribution of $M_{p\pi^0}$ and $M_{\bar{p}\pi^0}$ as can be seen in Fig. 2. To obtain the number of signal events, an unbinned maximum likelihood fit is performed to the $M_{p\pi^0}$ distribution by requiring $M_{\bar{p}\pi^0}$ to be within the signal region. The signal is described by the MC shape convoluted with a Gaussian function which represents the difference between data and MC in the resolution and mean value. The background is described with a second-order polynomial function. The mean and width of the Gaussian function and polynomial function parameters are all floated. Figure 3 shows the fitting of the $p\pi^0$ invariant mass distributions, where the red solid lines are the total fitting functions,

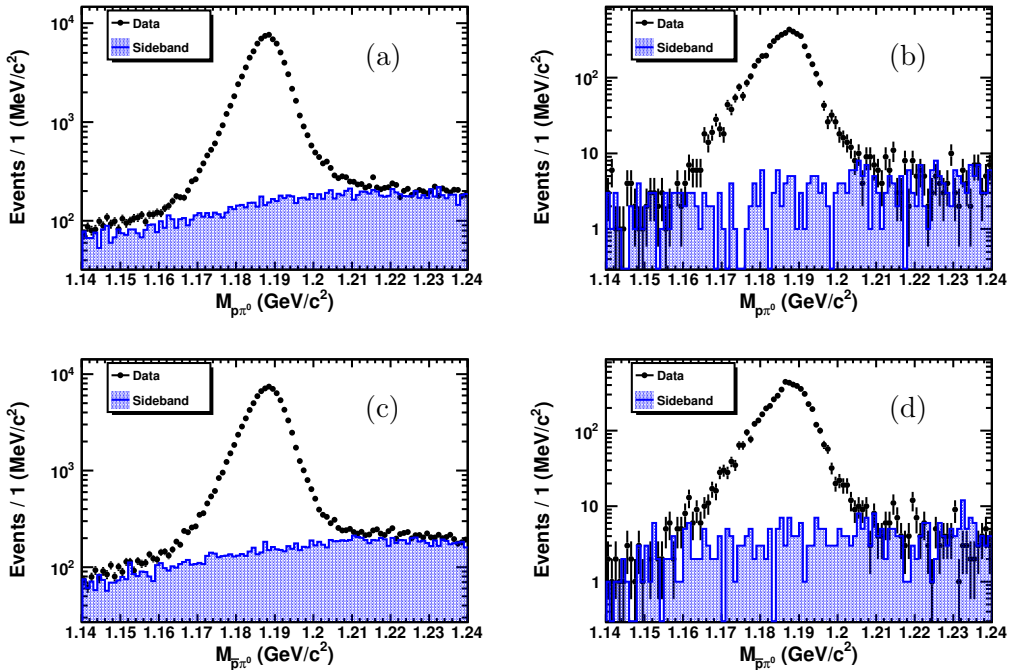


Figure 1. The invariant mass distributions of $p\pi^0$ (top) by requiring $M_{\bar{p}\pi^0}$ to be within the signal or sideband region and $\bar{p}\pi^0$ (bottom) by requiring $M_{p\pi^0}$ to be within the signal or sideband region. Left are $J/\psi \rightarrow \Sigma^+\bar{\Sigma}^-$ distributions and right are $\psi(3686) \rightarrow \Sigma^+\bar{\Sigma}^-$, where the black dots are data and the blue histograms are sideband contributions.

the red dashed lines are the signal functions and the blue dotted ones are the background functions.

The branching fraction of each channel is calculated according to

$$\mathcal{B}(\Psi \rightarrow \Sigma^+ \bar{\Sigma}^-) = \frac{N_{sig}}{\epsilon_{cor} \times \prod \mathcal{B}_i \times N_{\Psi}}, \quad (4.1)$$

where N_{sig} is the number of signal events determined by the fit, ϵ_{cor} is the corrected detection efficiency, generated according to the decay parameters measured in data but corrected for differences between data and MC simulation, $\prod \mathcal{B}_i$ is the product of the branching fractions of all the intermediate states in each channel and N_{Ψ} is the number of J/ψ or $\psi(3686)$ events [24, 25].

The corresponding numbers of signal events, detection efficiencies and branching fractions are listed in Table 2. The initial detection efficiencies are estimated with signal MC simulation. In the calculation of ϵ_{cor} , we take into account the difference between data and signal MC, obtained from control samples, which include the differences of detection efficiencies of the proton, anti-proton and π^0 . To study the tracking and PID efficiencies of the proton and anti-proton, the decay processes of $\Psi \rightarrow p\bar{p}\pi^+\pi^-$ are used to select the control samples of the proton or anti-proton. The proton efficiency ratios between MC and data are determined within different proton transverse-momentum and polar-angle regions. The ratios of anti-proton efficiency are also determined using the same method. To study the π^0 reconstruction efficiency, the control samples are selected with the processes of $\psi(3686) \rightarrow \pi^0\pi^0 J/\psi$, $J/\psi \rightarrow l^+l^-$ and $e^+e^- \rightarrow \omega\pi^0$ at $\sqrt{s} = 3.773$ GeV. The relative difference of the π^0 reconstruction efficiencies between MC and data obtained on the two datasets are consistent with each other and depend on π^0 momentum. The overall correction to the event selection efficiency is the product of correction factors of proton, anti-proton and π^0 in the related kinematic regions.

For the consistence study of 2009 and 2012 datasets, we study the branching fractions separately (only with statistical uncertainties). For J/ψ decay, the branching fractions are $(10.73 \pm 0.09) \times 10^{-4}$ and $(10.59 \pm 0.04) \times 10^{-4}$ for 2009 and 2012 separately, which are

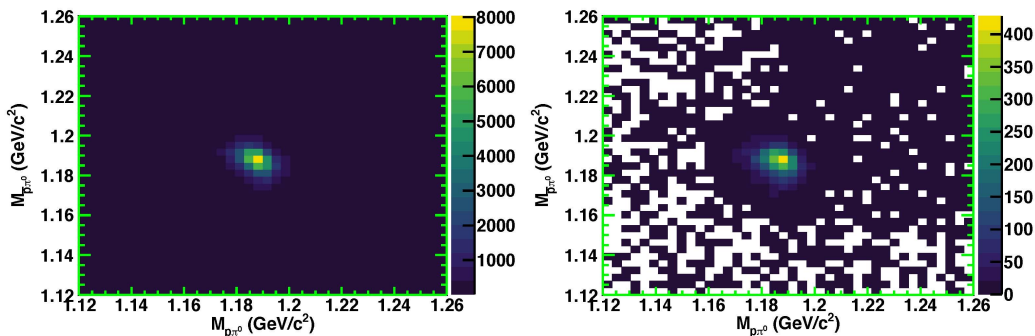


Figure 2. The two-dimensional distributions of $M_{p\pi^0}$ versus $M_{\bar{p}\pi^0}$. The left is J/ψ decay, and the right is $\psi(3686)$ decay.

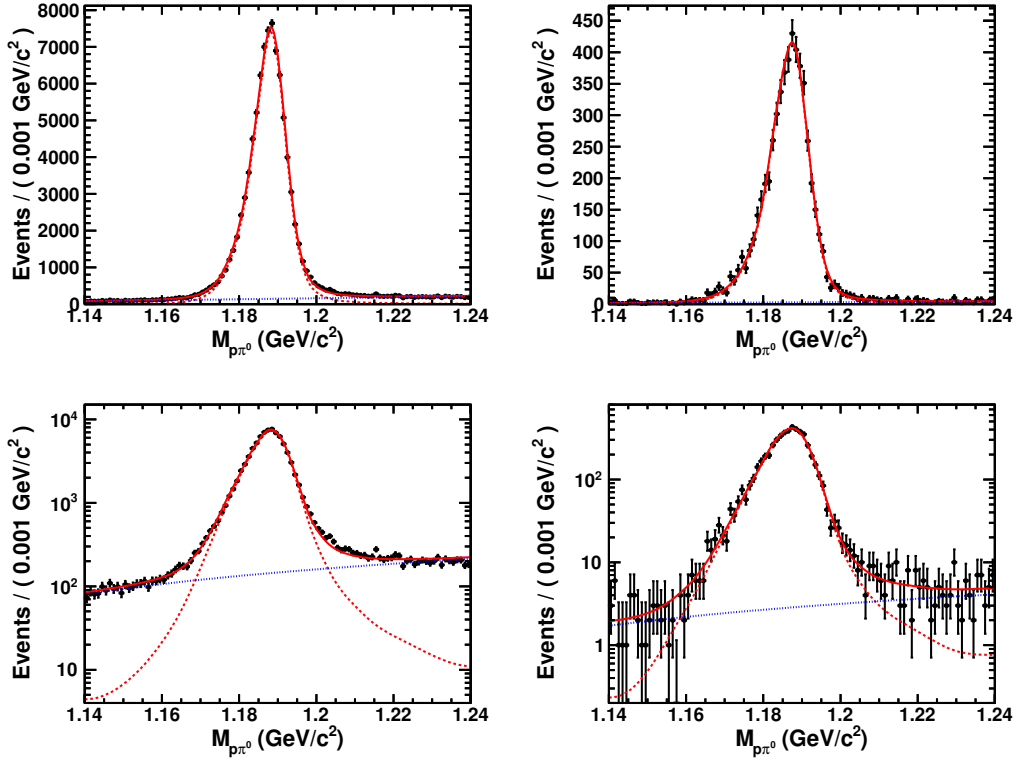


Figure 3. The Σ^+ invariant mass distributions with fit results superimposed. The left are for $J/\psi \rightarrow \Sigma^+\bar{\Sigma}^-$ and the right for $\psi(3686) \rightarrow \Sigma^+\bar{\Sigma}^-$. The bottom plots are in log scale. The red solid lines are the total fitting functions, the red dashed lines are the signal functions and the blue dotted ones are the background functions.

consistent with each other within 1.5 standard deviations. For $\psi(3686)$ decay, the branching fractions are $(2.57 \pm 0.07) \times 10^{-4}$ and $(2.50 \pm 0.04) \times 10^{-4}$ for 2009 and 2012 separately, which are consistent with each other within 1 standard deviations.

Table 2. The numbers of signal events, detection efficiencies and branching fractions of $\Psi \rightarrow \Sigma^+\bar{\Sigma}^-$, where the uncertainties are statistical only.

Channel	N_{sig}	$\epsilon_{cor}(\%)$	Branching fraction (10^{-4})
$J/\psi \rightarrow \Sigma^+\bar{\Sigma}^-$	86976 ± 314	24.1 ± 0.7	10.61 ± 0.04
$\psi(3686) \rightarrow \Sigma^+\bar{\Sigma}^-$	5447 ± 76	18.6 ± 0.5	2.52 ± 0.04

5 Systematic Uncertainties

The systematic uncertainties of the branching fraction measurements are mainly due to the difference of efficiency between data and simulation. The main sources come from the

difference in the detection efficiencies of charged and neutral particles in the final states. In addition, the detector resolution difference between data and MC also affects the efficiency via χ^2 requirement in the kinematic fit. Other sources, such as the fitting method, parameters of the generator and numbers of Ψ events, are also considered. Table 3 summarizes the sources of systematic uncertainties, which are discussed in further detail below.

5.1 MC efficiency correction for charged tracks

The tracking and PID efficiency differences between data and simulation for the proton and anti-proton have been studied in bins of transverse momentum and polar angle from control samples $\Psi \rightarrow p\bar{p}\pi^+\pi^-$. These differences are treated as correction factors to calculate the nominal efficiencies. The systematic uncertainties due to the limited statistics of the control samples are obtained by summing their relative uncertainties in different bins quadratically and are estimated to be 1.6% and 1.5% for J/ψ and $\psi(3686)$, respectively.

5.2 π^0 efficiency correction

Based on control samples of $\psi(3686) \rightarrow \pi^0\pi^0 J/\psi$, $J/\psi \rightarrow l^+l^-$ and $e^+e^- \rightarrow \omega\pi^0$ at $\sqrt{s} = 3.773$ GeV, the relative difference of the π^0 reconstruction efficiencies between data and MC has been obtained on the two datasets are consistent with each other. We studied the relative difference as a function of polar angle and momentum magnitude of π^0 , and found it to decrease linearly, $(0.06 - 2.41 \times p)\%$, as a function of momentum p . The detection efficiency differences obtained by varying the correction factor according to its uncertainty, $(\sqrt{0.76 \times p^2 + 1.15} + 0.39 \times p)\%$, are taken as the systematic uncertainties, which are 2.3% and 2.4% for J/ψ and $\psi(3686)$, respectively.

5.3 Decay parameters

The signal MC sample is generated according to a set of decay parameters which have been measured through multi-dimensional fitting of angular distributions, where polarization effects and decay asymmetry have been included [22]. Assuming no CP violation ($\alpha_0 = \bar{\alpha}_0$), three decay parameters α_Ψ , $\Delta\Phi_\Psi$ and α_0 are used for Ψ decay. We take the mean value and error matrix of these 3 parameters to build a 3 dimensional Gaussian distribution. Based on the 3 dimensional Gaussian distribution, we generate 1000 signal MC sample to evaluate the systematic uncertainty. The distributions of newly obtained efficiencies are fitted using a Gaussian function, and the widths are assigned as the systematic uncertainties, which are 0.6% and 0.7% for $J/\psi \rightarrow \Sigma^+\bar{\Sigma}^-$ and $\psi(3686) \rightarrow \Sigma^+\bar{\Sigma}^-$ respectively.

5.4 Fitting function

To estimate the uncertainties of the fitting function, we use the Crystal Ball function to describe the signal instead of the MC shape convoluted with a Gaussian function, and the differences are taken as the systematic uncertainties, 0.4% for $J/\psi \rightarrow \Sigma^+\bar{\Sigma}^-$ and 0.6% for $\psi(3686) \rightarrow \Sigma^+\bar{\Sigma}^-$.

5.5 Background estimation

There are two kinds of background events: peaking backgrounds and non-peaking backgrounds. For the peaking backgrounds, we neglect this contribution in calculating the branching fractions. Considering this contributions is less than 0.1%, we take 0.1% as conservative estimate for this kind of systematic uncertainties. For the non-peaking background, to estimate the uncertainties due to background modeling, we use the background shape determined by kernel density estimation from the sideband region of $M(\bar{p}\pi^0)$ instead of the second-order polynomial function. The differences are taken as the systematic uncertainties, 0.9% for $J/\psi \rightarrow \Sigma^+\bar{\Sigma}^-$ and 0.3% for $\psi(3686) \rightarrow \Sigma^+\bar{\Sigma}^-$.

5.6 $M(\bar{p}\pi^0)$ mass window selection

To select the signal events, we require the $1.17 < M(\bar{p}\pi^0) < 1.20$ GeV/ c^2 , which is a 30 MeV/ c^2 mass window. The systematic uncertainties related to $M(\bar{p}\pi^0)$ mass window selection are estimated by changing it to 24 MeV/ c^2 , 28 MeV/ c^2 , 32 MeV/ c^2 and 34 MeV/ c^2 , which are corresponding to $1.172 < M(\bar{p}\pi^0) < 1.198$ GeV/ c^2 , $1.171 < M(\bar{p}\pi^0) < 1.199$ GeV/ c^2 , $1.169 < M(\bar{p}\pi^0) < 1.201$ GeV/ c^2 and $1.168 < M(\bar{p}\pi^0) < 1.202$ GeV/ c^2 . The efficiencies and signal yields are re-evaluated with the varied windows to calculate the branching fractions. We compare the branching fractions with the nominal values and take the largest differences as the systematic uncertainties, which are 0.5% and 0.2% for J/ψ and $\psi(3686)$ decays respectively.

5.7 Kinematic fitting

To estimate the systematic uncertainty caused by the χ_{4C}^2 requirement, we obtain the χ_{4C}^2 distributions using the track correction method for the helix parameters [26]. By imposing the requirement of $\chi_{4C}^2 < 100$, the efficiencies are estimated, and compared with the nominal values. The differences, 0.1% for both J/ψ and $\psi(3686)$, are taken as the systematic uncertainties.

5.8 Branching fractions and numbers of J/ψ and $\psi(3686)$

The uncertainties related to the branching fractions of $\Sigma^+ \rightarrow p\pi^0$ and $\bar{\Sigma}^- \rightarrow \bar{p}\pi^0$ are taken as 1.2% according to the PDG [18]. The numbers of J/ψ and $\psi(3686)$ mesons are determined based on inclusive hadronic events, as described in [24, 25] with an uncertainty of 0.6% for J/ψ and 0.7% for $\psi(3686)$.

6 Summary

In summary, with 1310.6×10^6 J/ψ and 448.1×10^6 $\psi(3686)$ events collected by the BESIII detector, the branching fractions of J/ψ and $\psi(3686)$ decaying to $\Sigma^+\bar{\Sigma}^-$ are measured to be $(10.61 \pm 0.04 \pm 0.36) \times 10^{-4}$ and $(2.52 \pm 0.04 \pm 0.09) \times 10^{-4}$, respectively, and both are in agreement with the previous measurement [6, 11] within 2 standard deviations. The precision of the branching fraction of $J/\psi \rightarrow \Sigma^+\bar{\Sigma}^-$ is improved by a factor of 6.6 relative to the previous best measurement. The branching fraction ratio of the $\psi(3686)$ and J/ψ

Table 3. Systematic uncertainties

Source	$J/\psi \rightarrow \Sigma^+\bar{\Sigma}^-$ (%)	$\psi(3686) \rightarrow \Sigma^+\bar{\Sigma}^-$ (%)
Tracking and PID efficiency	1.6	1.5
π^0 reconstruction efficiency	2.3	2.4
Decay parameters	0.6	0.7
Fitting function	0.4	0.6
Peaking background	0.1	0.1
Non-peaking background	0.9	0.3
$M(\bar{p}\pi^0)$ mass window	0.5	0.2
Kinematic fitting	0.1	0.1
Branching fractions	1.2	1.2
Number of Ψ events	0.6	0.7
Total	3.4	3.3

decays is calculated to be $(23.8 \pm 1.1)\%$, where the statistical and systematic uncertainties are combined. The ratio is consistent with the previous measurement in the $\Sigma^0\bar{\Sigma}^0$ final states by the BESIII collaboration [27], and both violate the “12% rule”.

Acknowledgments

The BESIII collaboration thanks the staff of BEPCII and the IHEP computing center for their strong support. This work is supported in part by National Key R&D Program of China under Contracts Nos. 2020YFA0406300, 2020YFA0406400; National Natural Science Foundation of China (NSFC) under Contracts Nos. 11625523, 11635010, 11735014, 11822506, 11835012, 11935015, 11935016, 11935018, 11961141012, 12022510, 12025502, 12035009, 12035013, 12061131003; the Chinese Academy of Sciences (CAS) Large-Scale Scientific Facility Program; Joint Large-Scale Scientific Facility Funds of the NSFC and CAS under Contracts Nos. U1732263, U1832207; CAS Key Research Program of Frontier Sciences under Contract No. QYZDJ-SSW-SLH040; 100 Talents Program of CAS; INPAC and Shanghai Key Laboratory for Particle Physics and Cosmology; Sponsored by Shanghai Pujiang Program(20PJ1401700); ERC under Contract No. 758462; European Union Horizon 2020 research and innovation programme under Contract No. Marie Skłodowska-Curie grant agreement No 894790; German Research Foundation DFG under Contracts Nos. 443159800, Collaborative Research Center CRC 1044, FOR 2359, FOR 2359, GRK 214; Istituto Nazionale di Fisica Nucleare, Italy; Ministry of Development of Turkey under Contract No. DPT2006K-120470; National Science and Technology fund; Olle Engkvist Foundation under Contract No. 200-0605; STFC (United Kingdom); The Knut and Alice Wallenberg Foundation (Sweden) under Contract No. 2016.0157; The Royal Society, UK under Contracts Nos. DH140054, DH160214; The Swedish Research Council; U. S. Department of Energy under Contracts Nos. DE-FG02-05ER41374, DE-SC-0012069

References

- [1] G.R. Farrar and R. D. Jackson, Phys. Rev. Lett. **35**, 1416 (1975); B. L. Ioffe, Phys. Lett. B **63**, 425 (1976); A. I. Vainshtein and V. I. Zakharov, Phys. Lett. B **72**, 368 (1978); S. J. Brodsky and G. P. Lepage, Phys. Rev. D **24**, 2848 (1981).
- [2] S. Rudaz, Phys. Rev. D **14**, 298 (1976).
- [3] R. B. Ferroli, A. Mangoni, S. Pacetti and K. Zhu, Phys. Lett. B **799**, 135041 (2019).
- [4] K. Zhu, X. H. Mo and C. Z. Yuan, Int. J. Mod. Phys. A **30**, 1550148 (2015).
- [5] M. Tanabashi *et al.* (Particle Data Group), Phys. Rev. D **98** (2018), 030001.
- [6] M. Ablikim *et al.* (BES Collaboration), Phys. Rev. D **78**, 092005 (2008).
- [7] T. Appelquist and H. D. Politzer, Phys. Rev. Lett. **34**, 43 (1975); A. De Rujula and S. L. Glashow, Phys. Rev. Lett. **34**, 46 (1975).
- [8] M. E. B. Franklin, G. J. Feldman, G. S. Abrams, M. S. Alam, C. A. Blocker, A. Blondel, A. Boyarski, M. Breidenbach, D. L. Burke and W. C. Carithers, *et al.* Phys. Rev. Lett. **51**, 963 (1983)
- [9] Y. F. Gu and X. H. Li, Phys. Rev. D **63**, 114019 (2001); X. H. Mo, C. Z. Yuan and P. Wang, High Energy Physics and Nuclear Physics **31**, 686 (2007); N. Brambilla *et al.* (Quarkonium Working Group), Eur. Phys. J. C **71**, 1534 (2011); Q. Wang, G. Li and Q. Zhao, Phys. Rev. D **85**, 074015 (2012).
- [10] T. K. Pedlar *et al.* (CLEO Collaboration), Phys. Rev. D **72**, 051108 (2005).
- [11] S. Dobbs, K. K. Seth, A. Tomaradze, T. Xiao and G. Bonvicini, Phys. Rev. D **96**, 092004 (2017).
- [12] M. Ablikim *et al.* (BESIII Collaboration), Nucl. Instrum. Meth. A **614**, 345 (2010).
- [13] C. H. Yu *et al.*, Proceedings of IPAC2016, Busan, Korea, 2016.
- [14] M. Ablikim *et al.* (BESIII Collaboration), Chin. Phys. C **44**, 040001 (2020).
- [15] S. Agostinelli *et al.* (GEANT4 Collaboration), Nucl. Instrum. Meth. A **506**, 250 (2003); J. Allison *et al.*, IEEE Trans. Nucl. Sci. **53**, 270 (2006); J. Allison *et al.*, Nucl. Instrum. Meth. A **835**, 186-225 (2016).
- [16] S. Jadach, B. F. L. Ward and Z. Was, Comp. Phys. Commu. **130**, 260 (2000); Phys. Rev. D **63**, 113009 (2001).
- [17] D. J. Lange, Nucl. Instrum. Meth. A **462**, 152 (2001); R. G. Ping, Chin. Phys. C **32**, 599 (2008).
- [18] P.A. Zyla *et al.* [Particle Data Group], PTEP **2020**, no.8, 083C01 (2020)
- [19] J. C. Chen, G. S. Huang, X. R. Qi, D. H. Zhang and Y. S. Zhu, Phys. Rev. D **62**, 034003 (2000); R. L. Yang, R. G. Ping and H. Chen, Chin. Phys. Lett. **31**, 061301 (2014).
- [20] E. Barberio, B. van Eijk and Z. Was, Comput. Phys. Commun. **66**, 115-128 (1991); E. Richter-Was, Phys. Lett. B **303**, 163 (1993); P. Golonka and Z. Was, Eur. Phys. J. C **45**, 97-107 (2006).
- [21] G. Fäldt and A. Kupsc, Phys. Lett. B **772**, 16 (2017).
- [22] M. Ablikim *et al.* (BESIII Collaboration), Phys. Rev. Lett. **125**, 052004 (2020).

- [23] X. Y. Zhou, S. X. Du, G. Li and C. P. Shen, *Comput. Phys. Commun.* **258**, 107540 (2021).
- [24] M. Ablikim *et al.* (BESIII Collaboration), *Chin. Phys. C* **41**, 013001 (2017).
- [25] M. Ablikim *et al.* (BESIII Collaboration), *Chin. Phys. C* **42**, 023001 (2018).
- [26] M. Ablikim *et al.* (BESIII Collaboration), *Phys. Rev. D* **87**, 012002 (2013).
- [27] M. Ablikim *et al.* (BESIII Collaboration), *Phys. Rev. D* **95**, 052003 (2017).